Published OnlineFirst May 18, 2010; DOI: 10.1158/0008-5472.CAN-09-3704

Cancer Research

Superior *In vivo* Efficacy of Afucosylated Trastuzumab in the Treatment of HER2-Amplified Breast Cancer

Teemu T. Junttila, Kathryn Parsons, Christine Olsson, Yanmei Lu, Yan Xin, Julie Theriault, Lisa Crocker, Oliver Pabonan, Tomasz Baginski, Gloria Meng, Klara Totpal, Robert F. Kelley, and Mark X. Sliwkowski

Abstract

The enhancement of immune effector functions has been proposed as a potential strategy for increasing the efficacy of therapeutic antibodies. Here, we show that removing fucose from trastuzumab (Herceptin) increased its binding to FcγRIIIa, enhanced antibody-dependent cell-mediated cytotoxicity, and more than doubled the median progression-free survival when compared with conventional trastuzumab in treating preclinical models of HER2-amplified breast cancer. Our results show that afucosylated trastuzumab has superior efficacy in treating *in vivo* models of HER2-amplified breast cancer and support the development of effector function–enhanced antibodies for solid tumor therapy. *Cancer Res; 70(11); 4481–9. ©2010 AACR.*

Introduction

Herceptin (trastuzumab) is a humanized antibody for treating HER2/ErbB2-overexpressing breast cancer. Trastuzumab was initially approved for the treatment of women with HER2-positive metastatic breast cancer in combination with standard cytotoxic chemotherapy (1) and as a monotherapy (2, 3). Multiple studies have been completed in several large adjuvant or early breast cancer trials for HER2-positive breast cancer (4). A survival benefit was noted after only 2 years of follow-up, which is impressive in breast cancer (4). Multiple mechanisms of action are thought to contribute to the tumor-inhibitory effect of trastuzumab. Binding of trastuzumab to HER2 has a direct inhibitory effect on HER2-amplified tumor cells. Trastuzumab disrupts the ligand-independent HER2-HER3 interaction resulting in rapid inhibition of HER3/PI3K/AKT signaling (5). Ultimately, this leads to an increase in the CDK2 inhibitor, p27, resulting in cell cycle arrest of the cancer cells (5–8). Another primary effect on tumor cells is the ability of trastuzumab to inhibit HER2 ectodomain shedding (9), which may have therapeutic significance. Trastuzumab is also known to have synergistic effects when combined with chemotherapy (10).

In addition to directly inhibiting tumor cell signaling, trastuzumab can also mediate the effector functions of immune cells through the constant region (Fc) of the antibody. As a humanized IgG_1, it binds to Fcγ receptor III (RIII) and is a potent mediator of antibody-dependent cell-mediated cytotoxicity (ADCC). The ability of trastuzumab to mediate ADCC is strictly related to HER2 density (11). Tumor cells that overexpress HER2 are observed to have 100-fold more HER2 on their cell surface than normal adjacent breast epithelial cells (12). As a result, trastuzumab mediates ADCC very effectively against target cell lines that overexpress HER2 but displays only background activity against cells that express normal levels of HER2. Depleting trastuzumab effector functions by Fc modification or deleting the FcγR functions from the mouse results in significant reduction of trastuzumab efficacy, demonstrating the importance of immune effector functions in trastuzumab response (13). Clinical relevance for effector functions of Herceptin is supported by a report demonstrating that trastuzumab efficacy correlated with the high-affinity FcγRIII genotype (V/V; ref. 14) similar to rituximab-treated patients (15). Furthermore, increased tumor-associated natural killer (NK) cells and lytic capacity of effector cells were detected after trastuzumab treatment (16–18), and trastuzumab response correlated with high *in vitro* ADCC (17, 18) and immune cell infiltration (17).

Together, the aforementioned studies provide a biological and clinical rationale for a strategy in which increasing trastuzumab-FcγRIIIa affinity could enhance therapeutic benefit. Currently, no published reports have shown that enhancing FcγR affinity results in enhanced *in vivo* efficacy for the treatment of established, nonhematologic tumors. Although promising results are described in a few published reports in which treatment commenced at the same time as tumor cell inoculation (13, 19, 20), these studies leave open the question of whether the observed outcomes were due to the effects on tumor implantation. The primary aim of the present study is to determine whether the efficacy of trastuzumab in suppressing the growth of established tumors is augmented by increasing FcγR binding affinity.

Authors' Affiliation: Genentech, Inc., South San Francisco, California

Note: Supplementary data for this article are available at Cancer Research Online (http://cancerres.aacrjournals.org/).

Corresponding Author: Mark X. Sliwkowski, Genentech, Inc., 1 DNA Way, Mailstop 72, South San Francisco, CA 94080. Phone: 650-225-1247; Fax: 650-467-8195; E-mail: marks@gene.com.

doi: 10.1158/0008-5472.CAN-09-3704

Published OnlineFirst May 18, 2010; DOI: 10.1158/0008-5472.CAN-09-3704

Materials and Methods

Cell lines

Breast cancer cell line BT-474-M1 is an *in vivo*–passaged subclone of BT-474 (American Type Culture Collection; ref. 13). MCF7-neo/HER2 cells were established at Genentech, Inc. KPL-4 breast cancer cells were obtained from J. Kurebayashi (Department of Breast and Thyroid Surgery, Kawasaki Medical School, Kurashiki, Okayama, Japan; ref. 21). SKBR-3 and MCF-10A cells were from American Type Culture Collection. Cell lines were maintained in high-glucose DMEM/Ham's F-12 (50:50) supplemented with 10% fetal bovine serum and 2 mmol/L of L-glutamine.

Analysis of N-linked oligosaccharides

The oligosaccharide profiles of the antibodies were analyzed by matrix-assisted laser desorption/ionization time-of-flight mass spectrometry, as previously described (22).

Fcγ receptor binding ELISA

Soluble human FcγRI, FcγRIIA, FcγRIIB, FcγRIIIA(F158), and FcγRIIIA(V158) (ref. 23), and mouse FcγRI, FcγRII, and FcγRIIIA (Genentech) were expressed in Chinese hamster ovary (CHO) cells (mFcγRI and mFcγRII in 293 cells) as recombinant fusion proteins with Gly-His6–glutathione *S*-transferase at the COOH terminus of the extracellular domain of the receptor α chains. Soluble mouse FcγRIV was expressed in CHO cells as a recombinant fusion protein with Gly-His8 at the COOH terminus of the extracellular domain of the receptor α chains (Genentech). MaxiSorp 384-well microwell plates (Nunc) were coated with 2 μg/mL of anti–glutathione *S*-transferase (clone 8E2.1.1; Genentech) or anti-His (penta his antibody, for mouse FcγRIV; Qiagen) in 50 mmol/L of carbonate buffer (pH 9.6), at 4°C overnight followed by a wash (PBS containing 0.05% polysorbate; pH 7.4). Plates were blocked for 1 hour in room temperature with PBS containing 0.5% bovine serum albumin (BSA) and washed. Fcγ receptor [0.25 μg/mL, in PBS containing 0.5% BSA, and 0.05% polysorbate 20 (pH 7.4) in assay buffer] was incubated in plates for 1 hour followed by a wash. To measure binding to the high-affinity FcγRI, IgG antibodies (0.0085–500 ng/mL in 3-fold serial dilution) in assay buffer were added to the plates. To measure binding to the low-affinity FcγRII, FcγRIII, and FcγRIV, IgG antibodies were first incubated with goat *F*(ab′)2 anti-κ antibody (MP Biomedicals) at a 1:2 (w/w) ratio for 1 hour to form antibody complexes. Complexed IgG antibodies (0.42–25,000 ng/mL in 3-fold serial dilution) in assay buffer were added to the plates, incubated for 2 hours, and washed. Bound IgG was detected after 1 hour of incubation with peroxidase-labeled goat *F*(ab′)2 anti-human IgG *F*(ab′)2 (Jackson ImmunoResearch) in assay buffer followed by a wash, incubation with substrate (3′,5,5′-tetramethyl benzidine; Kirkegaard & Perry Laboratories), and termination with 1 mol/L of phosphoric acid. The absorbance (450 nm) at the midpoint of the standard curve (mid-OD) was calculated. The corresponding concentrations of standard and samples at this mid-OD were determined from the titration curves using a four-parameter nonlinear regression curve-fitting program (XLfit).

In vitro ADCC

In vitro ADCC assays were performed as previously described (24). In short, peripheral blood mononuclear cells (PBMC) were separated from the blood of normal volunteers using lymphocyte separation medium (MP Biomedicals). The NK cells were enriched from the PBMCs using anti-CD56 microbeads (Miltenyi Biotec). Target cells (1×10^4) were preincubated with antibodies for 30 minutes in 37°C in serum-free RPMI 1640 supplemented with 0.1% BSA before adding the effector cells in a 25:1 E/T ratio (10:1 when NKs were used as effectors). The cells were incubated for an additional 4 hours before detecting death by measuring the lactate dehydrogenase activity from the medium using Cytotoxicity Detection Kit (LDH; Roche). All measurements were done in quadruplicate. The percentage of cytotoxicity was calculated as follows: % cytotoxicity (experimental lysis – spontaneous effector lysis – spontaneous target lysis) / (maximum target lysis – spontaneous target lysis) × 100.

HER2 binding

Nunc BreakApart Immunomodule plates (Nunc) were coated with 20 ng/mL of HER2-ECD-Ig fusion protein in 50 mmol/L of HEPES (pH 8.2), and 150 mmol/L of NaCl overnight at 4°C. Nonspecific binding was blocked with 2 mg/mL of BSA, 25 mmol/L of Tris (pH 7.5), and 150 mmol/L of NaCl for 2 hours at room temperature. Wells were washed thrice with assay buffer [2 mg/mL BSA and 10 mmol/L HEPES (pH 7.2) in RPMI]. The competitive binding reaction with a dilution series of nonlabeled competitor antibodies and constant ^{125}I-trastuzumab was carried out for 2 hours at room temperature. The ^{125}I-trastuzumab bound to HER-2 was then detected by a gamma counter and the data were analyzed using the nonlinear regression method of Munson and Rodbard (25). All measurements were done in quadruplicate.

Analysis of PI3K/AKT pathway activation

Cells were rinsed with PBS and lysed with nondenaturing lysis buffer including 1% Triton (Cell Signaling Technology). Lysates were cleared of insoluble material by centrifugation. AKT phosphorylation was detected by ELISA detecting phosphorylated Ser^{473} (Cell Signaling Technology).

Cell proliferation

Proliferation/viability of cells was detected using CellTiter-Glo Luminescent Cell Viability Assay (Promega). For the assay, 5×10^3 cells were plated on 96-well plates and incubated overnight for cell attachment before 6 days of treatment with the antibodies. All measurements were done in triplicate.

Mice

Rag2$^{-/-}$ (BALB/c; Taconic) mice were crossbred to *FcγRI/III*$^{-/-}$ (CD64/CD16 double KO, BALB/c, kindly provided by S. Verbeek; refs. 26, 27), resulting in FcγRI/III/Rag2$^{-/-}$ mice, which were then crossbred to human FcγRIIIa transgenic

Published OnlineFirst May 18, 2010; DOI: 10.1158/0008-5472.CAN-09-3704

Table 1. Oligosaccharide profile of afucosylated trastuzumab

Glycan structure	Total AB (%)	
	Trastuzumab	Afucosylated
	5	
	2	
	8.5	87
	43	
	8	13
	28	
	3	
	2.5	
Total	100	100
Fucosylated	76	0

NOTE: ▲, fucose (Fuc); ◆, galactose (Gal); ⬭, Mannose (Man); ■, *N*-acetylglucosamine (GlcNAc).

mice (Bl-6, kindly provided by J. Ravetch; ref. 28) to obtain *FcγRI*$^{-/-}$*FcγRIII*$^{-/-}$*RAG2*$^{-/-}$*Tg* (human FcγRIIIa) mice. The human transgene is the low-affinity FcγRIIIa-F158 allele (Supplementary Fig. S2B). Severe combined immunodeficiency (SCID)-beige mice were obtained from Charles River Labs.

Pharmacokinetic studies

Pharmacokinetic studies were performed as previously described (29). In short, a single i.v. 10 mg/kg dose of trastuzumab or afucosylated trastuzumab was injected to *FcγRI*$^{-/-}$*FcγRIII*$^{-/-}$*RAG2*$^{-/-}$*Tg* (human FcγRIIIa) mice. Serum samples (n = 4/time point) were collected by retro-orbital bleed or cardiac stick after administration of the antibodies (time points: 3 minutes, 1 and 5 hours, and 1, 3, 7, 14, and 28 days). Samples were assayed for trastuzumab by HER2 binding ELISA (29), in which a HER2 extracellular domain coated to a microtiter plate was used to capture the humanized anti-HER2 antibodies in circulation. Time concentration data were analyzed using compartmental pharmacokinetic analysis (Model 8, WinNonlin-Pro v3.2; Pharsight Corporation).

In vivo drug efficacy

To address the requirement of FcγR interaction in the trastuzumab response using T-D265A, SCID-beige mice (Charles River Labs) were used. For afucosylated trastuzumab efficacy studies, *FcγRI*$^{-/-}$*FcγRIII*$^{-/-}$*RAG2*$^{-/-}$*Tg* (human FcγRIIIa) mice were used. Mice xenografted with MCF7-neo/HER2 cells were supplemented with subcutaneous estrogen pellets (0.36 mg, 60-day release; Innovative Research of America) 3 days prior to cell inoculation. Five million MCF7-neo/HER2 cells or 3 million KPL-4 cells were injected into the mammary fat pad in a 1:1 HBSS-matrigel suspension (BD Matrigel, BD Biosystems). When tumor volumes reached 100 to 300 mm^3, mice were randomly grouped into treatment cohorts. Dosing is described in the figure legends. Tumor volumes were calculated using the formula: (mm^3) = ($L \times W^2$) × 0.5.

Table 2. Binding of afucosylated trastuzumab to human and mouse FcγR

	Relative affinity to mouse FcγR							
	I		II		III		IV	
	Mid-OD*	Fold†	Mid-OD*	Fold†	Mid-OD*	Fold†	Mid-OD*	Fold†
Trastuzumab	197.0	1	4,435	1	6,045	1	138	1
Afucosylated	231.0	0.9	3,690	1.2	6,403	0.9	71	1.9

	Relative affinity to human FcγR									
	I		IIa		IIb		IIIa-F158		IIIa-V158	
	Mid-OD*	Fold†	Mid-OD*	Fold†	Mid-OD*	Fold†	Mid-OD*	Fold†	Mid-OD*	Fold†
Trastuzumab	12.7	1	1,783	1	5,851	1	2,156	1	263	1
Afucosylated	9.2	1.4	1,639	1.1	3,963	1.5	74	29.2	40	6.5

*In ng/mL.
†Fold = mid-OD trastuzumab/mid-OD afucosylated.

Published OnlineFirst May 18, 2010; DOI: 10.1158/0008-5472.CAN-09-3704

Results

Afucosylated trastuzumab has increased affinity to human FcγRIIIa which results in enhanced ADCC

We produced 100% fucose-free (afucosylated trastuzumab) trastuzumab in *FUT8*$^{-/-}$ CHO cells (30). The *FUT8* gene encodes 1,6-fucosyltransferase, which catalyzes the transfer of fucose from GDP-fucose to *N*-acetylglucosamine. The oligosaccharide profile of the antibodies was determined by matrix-assisted laser desorption/ionization time-of-flight analysis, which confirmed the lack of fucose (Table 1). The relative affinity of afucosylated trastuzumab was analyzed by FcγR binding ELISA. Binding to FcγRIIIa-F158 and FcγRIIIa-V158 increased by 29-fold and 6.5-fold, respectively (Table 2). Binding to human FcγRI, FcγRIIa, and FcγRIIb was not markedly altered, indicating that afucosylated trastuzumab has selective enhanced affinity for FcγRIII (Table 2). Similarly, binding to mouse FcγRI, FcγRII, or FcγRIII was not increased and only a minor increase was detected in relative affinity to FcγRIV (Table 2). The increases in binding affinity to mFcγRIV and huFcγRIIIa-V158 were similar (3.3- and 6.2-fold decreased K_D, respectively; data not shown) when binding was measured using surface plasmon resonance–based technology (Biacore).

Afucosylated trastuzumab showed increased *in vitro* ADCC. The ability to mediate ADCC improved 1.9- to 7.2-fold (EC_{50}; $n = 5$) when F/F effectors were used and 2.1- to 7.7-fold ($n = 5$) when V/V donors were used (Fig. 1A; data not shown). A representative experiment using F/F effector cells is presented in Fig. 1A. ADCC activity increase was statistically significant in 0.01 to 0.1 ng/mL antibody doses (Fig. 1A; *t* test). Despite the effector cell donor–dependent variability, the EC_{50} was consistently lower for afucosylated trastuzumab in each assay. ADCC activity of PBMCs was mediated by NK cells (Fig. 1A). When purified NK cells from F/F donors were used as effector cells, an 11.3-fold enhancement in ADCC was observed for afucosylated trastuzumab (Fig. 1A). Afucosylated trastuzumab did not mediate ADCC of MCF-10A cells which express low/normal levels of HER2 even at high antibody concentrations and using V/V effectors cells (Supplementary Fig. S1A). Together, these results show that afucosylated trastuzumab has increased affinity for human FcγRIIIa, which results in enhanced ADCC.

Afucosylated trastuzumab retains FcγR-independent functions of trastuzumab

In addition to the ability to mediate ADCC, trastuzumab has a direct effect on tumor cell signaling which causes cell

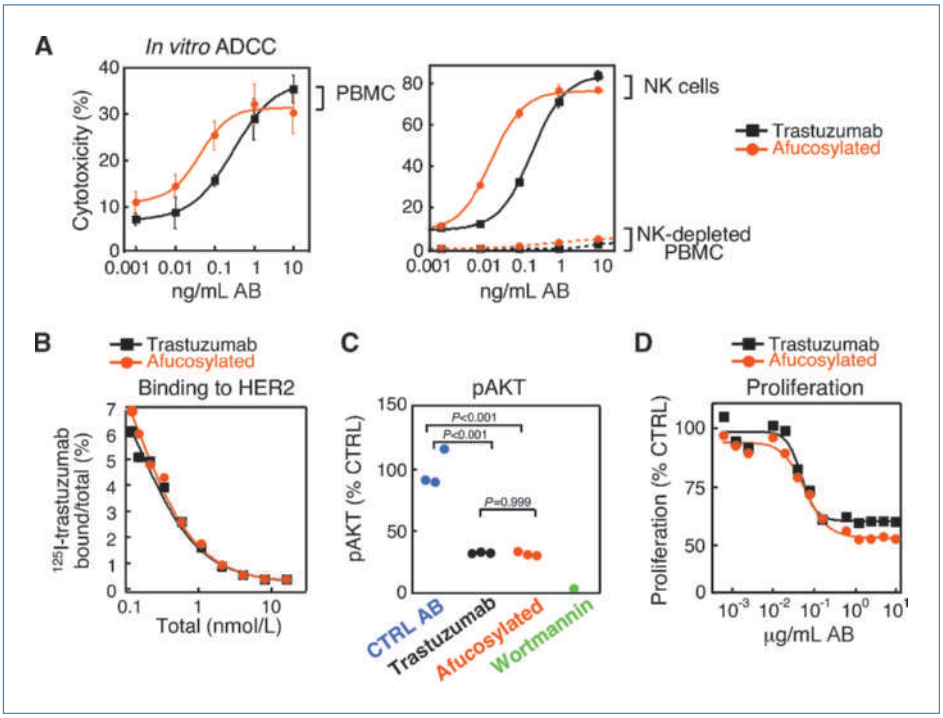

Figure 1. *In vitro* characterization of afucosylated trastuzumab. A, increased affinity to human FcγRIIIa results in enhanced ADCC. The ability of trastuzumab (black symbols) and afucosylated trastuzumab (red symbols) to mediate *in vitro* ADCC by FcγRIIIa-F158 homozygous PBMCs (left), NK cells or NK cell–depleted PBMCs (right) was measured using assay detecting LDH released from lysed cells. HER2-amplified BT474-M1 cells were used as target cells in a 25:1 effector/target ratio (10:1 when NK cells were used as effectors). B to D, removal of fucose does not affect FcγR-independent properties of trastuzumab. B, binding to recombinant extracellular domain of human HER2 was determined by competition binding of ^{125}I-trastuzumab with nonlabeled trastuzumab or afucosylated trastuzumab. C, HER2-amplified SKBR-3 cells were treated for 1 h with antibodies (10 µg/mL) or Wortmannin (1 µmol/L). AKT phosphorylation was measured by ELISA detecting phosphorylated Ser^{473}. Statistical significance between groups was determined using Dunnett's test. D, proliferation of SKBR-3 cells was analyzed after 6 days of treatment with trastuzumab or afucosylated trastuzumab using CellTiter-Glo Luminescent Cell Viability Assay.

Published OnlineFirst May 18, 2010; DOI: 10.1158/0008-5472.CAN-09-3704

cycle arrest and inhibition of proliferation. To confirm that carbohydrate modification does not affect HER2 binding, we competed the binding of radioiodinated trastuzumab to HER2 ECD by adding increasing concentrations of noniodinated antibody (trastuzumab or afucosylated trastuzumab) in the reaction (Fig. 1B). The calculated affinities of antibodies were similar for trastuzumab and afucosylated trastuzumab (K_D, 0.13 ± 0.04 and 0.12 ± 0.03 nmol/L, respectively), indicating that lack of fucose does not affect HER2 binding.

To explore the antisignaling properties, SKBR-3 cells were treated with trastuzumab or the afucosylated variant. Treatment with 10 μg/mL of trastuzumab or afucosylated trastuzumab caused a 69% to 66% reduction in pAKT after 60 minutes of treatment (Fig. 1C). No difference was detected in the effects of afucosylated and conventional trastuzumab treatment ($P = 0.99$; Dunnetts'). SKBR-3 proliferation was measured after 6 days of treatment. Both antibodies caused approximately 50% maximal reduction in proliferation (Fig. 1D). The EC_{50} values were 52 ± 8 and 61 ± 9 ng/mL for trastuzumab and afucosylated trastuzumab, respectively. Together, these results confirm that the lack of fucose does not affect the FcγR-independent functions of trastuzumab. These functions include HER2 binding, the immediate inhibition of the PI3K pathway, and sustained inhibition of tumor cell proliferation.

Pharmacokinetic properties of afucosylated trastuzumab

Removal of fucose does not affect IgG binding to FcRn (23). However, carbohydrate composition or increased FcγR affinity might have an effect on target-independent clearance or drug disposition of the antibody (31). To address this question, we performed pharmacokinetic analysis of afucosylated trastuzumab. For this purpose, the systemic disposition of trastuzumab and afucosylated trastuzumab was evaluated in *FcγRI*$^{-/-}$*FcγRIII*$^{-/-}$*RAG2*$^{-/-}$*Tg* (human FcγRIIIa) mice following a single i.v. dose (10 mg/kg). Serum samples (n = 4/time point) were analyzed for anti-HER2 antibodies 3 minutes to 28 days after administration of the antibodies. Both molecules displayed biphasic systemic disposition, with a rapid initial phase and a prolonged terminal phase (Fig. 2). Afucosylated trastuzumab displayed increased clearance (9.0 versus 6.8 mL/d/kg), decreased terminal half-life (10.1 versus 13.1 days), and decreased $AUC_{0\text{-inf}}$ (1,118 versus 1,463 d × μg/mL) relative to trastuzumab (Fig. 2). Both groups displayed a central volume of distribution values (V_1) that approximated mouse plasma volume. Taken together, these results show that afucosylated trastuzumab exhibited moderately altered pharmacokinetic dispositions compared with trastuzumab, slightly faster elimination from the circulation, and a modest reduction in half-life.

FcγR interaction is required for trastuzumab response in the treatment of established KPL-4 tumor xenografts

The KPL-4 breast cancer cell line harbors HER2 amplification (21) but does not respond to trastuzumab *in vitro* in a proliferation assay (5). A "hotspot" *PIK3CA* mutation (H1047R) generates constitutive PI3K/AKT signals and is

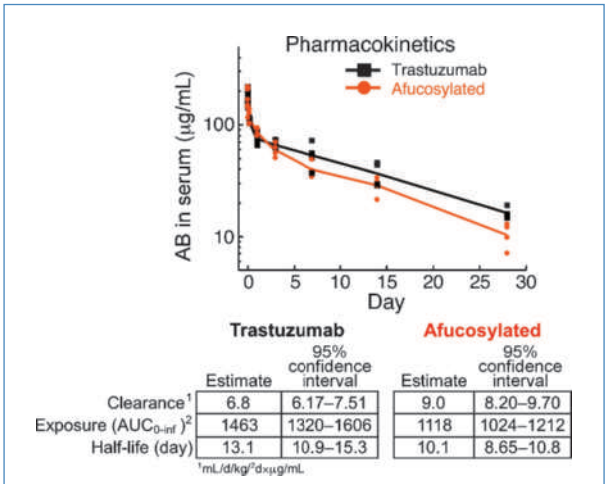

	Trastuzumab		Afucosylated	
	Estimate	95% confidence interval	Estimate	95% confidence interval
Clearance[1]	6.8	6.17–7.51	9.0	8.20–9.70
Exposure ($AUC_{0\text{-inf}}$)[2]	1463	1320–1606	1118	1024–1212
Half-life (day)	13.1	10.9–15.3	10.1	8.65–10.8

[1]mL/d/kg [2]d×μg/mL

Figure 2. Pharmacokinetic profile of afucosylated trastuzumab. A single i.v. 10 mg/kg dose of trastuzumab (black symbols) or afucosylated trastuzumab (red symbols) was injected to *FcγRI*$^{-/-}$*FcγRIII*$^{-/-}$*RAG2*$^{-/-}$Tg (human FcγRIIIa) mice. Serum samples were assayed for trastuzumab by ELISA.

the likely cause for the trastuzumab insensitivity. However, KPL-4 cells are sensitive to the FcγR-mediated trastuzumab activity similar to BT474-M1 (Supplementary Fig. S1B). Despite the inability of trastuzumab to inhibit KPL-4 cell proliferation, KPL-4 tumor xenografts respond to trastuzumab when treated with three weekly 15 mg/kg doses (Fig. 3A, left). To confirm that the *in vivo* response is dependent on FcγR interaction, we also treated mice with the D265A mutant of trastuzumab (T-D265A). The single alanine substitution impairs binding of trastuzumab in all human and mouse FcγR (13). Treatment of mice with T-D265A resulted in almost complete loss of response (Fig. 3A, left), confirming that trastuzumab response in the treatment of KPL-4 tumors were due to the FcγR-dependent effects of trastuzumab.

Increased *in vivo* efficacy of afucosylated trastuzumab

To assess the efficacy of afucosylated trastuzumab *in vivo*, we treated established KPL-4 xenografts grown in the mammary fat pads of SCID-beige mice with three weekly 10 mg/kg doses of trastuzumab or afucosylated trastuzumab. Although both trastuzumab and afucosylated trastuzumab inhibited the tumor growth ($P < 0.001$ and $P = 0.003$, respectively; log rank test), no difference was seen between the antibodies ($P = 0.48$; log rank test), indicating that the modest increase in binding affinity to FcγRIV was not sufficient to result in increased efficacy (Fig. 3A, right).

To further evaluate the activity of the afucosylated trastuzumab variant, we generated *FcγRI*$^{-/-}$*FcγRIII*$^{-/-}$*RAG2*$^{-/-}$*Tg* (human FcγRIIIa) mice that lack murine FcγRI (27) and FcγRIII (26) and express the human FcγRIIIa transgene (28). The transgene expression is controlled by the human FcγRIIIa promoter and is expressed in NK cells and macrophages (28). Expression of the transgene in mice was

Published OnlineFirst May 18, 2010; DOI: 10.1158/0008-5472.CAN-09-3704

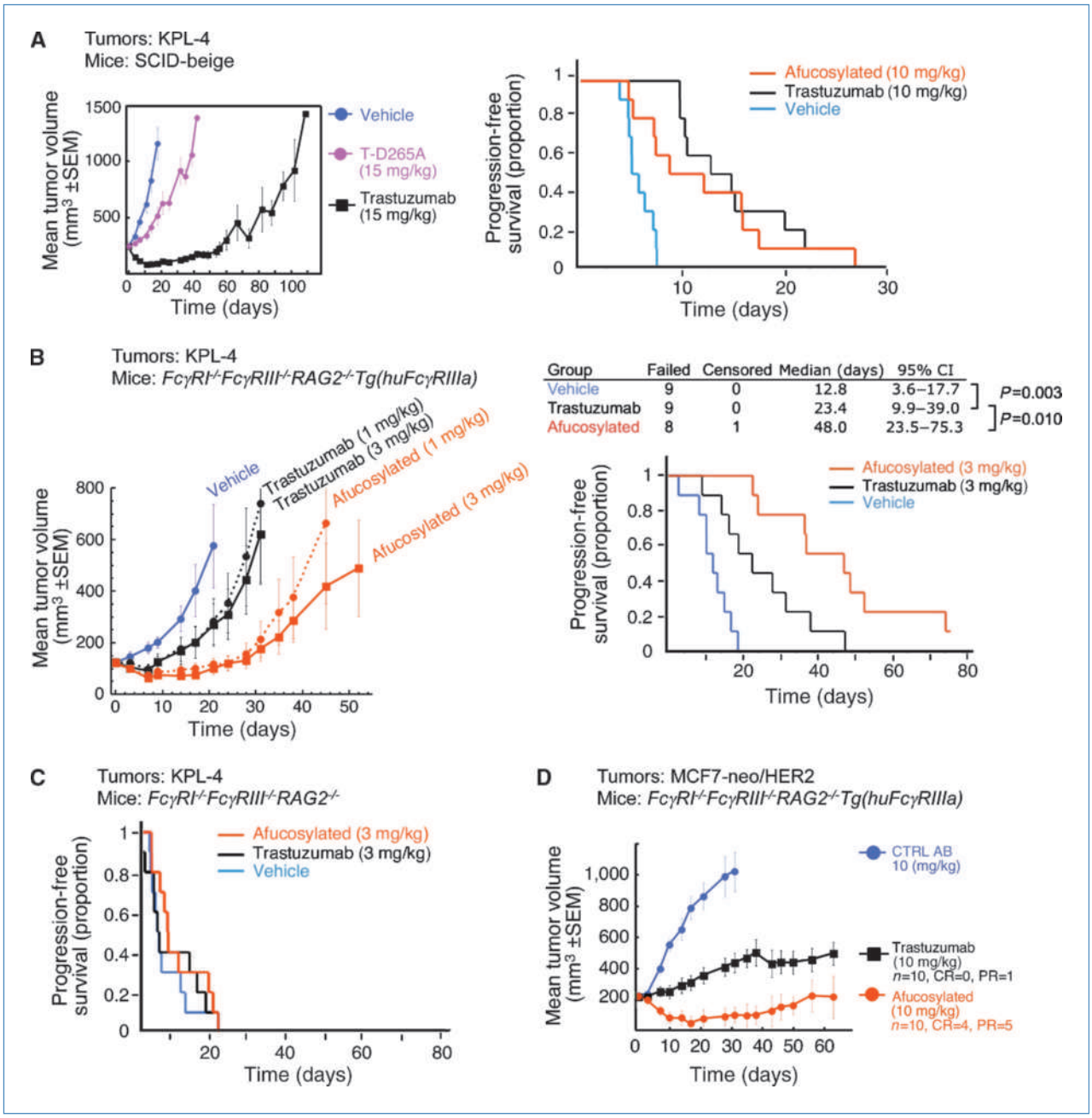

Figure 3. Superior *in vivo* efficacy of afucosylated trastuzumab compared with trastuzumab. A, FcγR interaction is required for trastuzumab response in the treatment of KPL-4 tumor xenografts (left). Established KPL-4 tumor xenografts in SCID-beige mice were treated with vehicle (blue), trastuzumab (black), or a trastuzumab variant incapable of FcγR binding (T-D265A; magenta). Intraperitoneal 15 mg/kg, 1×/wk × 3 dosing was started at day 0. A loading dose of 30 mg/kg was administered on the first injection (n = 8). Efficacy of afucosylated trastuzumab in SCID-beige mice: pre-established KPL-4 tumors were treated with vehicle (blue), trastuzumab (black), or afucosylated trastuzumab (red). Intraperitoneal 10 mg/kg, 1×/wk × 3 dosing was started at day 0 (right). A loading dose of 20 mg/kg was administered on the first injection (n = 10). Time to progression: tumor $V = 2 \times V$ on day 0. B, KPL-4 tumor xenograft bearing *FcγRI*$^{-/-}$*FcγRIII*$^{-/-}$*RAG2*$^{-/-}$*Tg* (human FcγRIIIa) mice were treated with vehicle (blue), trastuzumab (black), or afucosylated trastuzumab (red). A single 1 mg/kg (dotted lines) or 3 mg/kg (solid lines) dose was administered i.v. at day 0 (n = 9; left). Progression-free survival for *FcγRI*$^{-/-}$*FcγRIII*$^{-/-}$*RAG2*$^{-/-}$*Tg* (human FcγRIIIa) mice bearing KPL-4 tumors treated with vehicle (blue), trastuzumab (3 mg/kg, black), or afucosylated trastuzumab (3 mg/kg, red; n = 9). Dose was administered i.v. at day 0 (right). Time to progression: tumor $V = 2 \times V$ on day 0. Statistical significance was determined using log rank test. C, KPL-4 tumor xenograft bearing *FcγRI*$^{-/-}$*FcγRIII*$^{-/-}$*RAG2*$^{-/-}$ mice were treated with vehicle (blue), trastuzumab (black), or afucosylated trastuzumab (red). Intravenous 3 mg/kg, 1×/wk × 3 dosing was started at day 0 (n = 10). Time to progression: tumor $V = 2 \times V$ on day 0. D, MCF7-neo/HER2 tumor xenograft bearing *FcγRI*$^{-/-}$*FcγRIII*$^{-/-}$*RAG2*$^{-/-}$*Tg* (human FcγRIIIa) mice were treated with control AB (blue), trastuzumab (black), or afucosylated trastuzumab (red). Intravenous 10 mg/kg, 1×/wk × 3 dosing was started at day 0. A loading dose of 20 mg/kg was administered on the first injection. CR, complete response (no detectable tumor); PR, partial response (tumor volume reduced <50% of day 0; n = 10).

Published OnlineFirst May 18, 2010; DOI: 10.1158/0008-5472.CAN-09-3704

confirmed by quantitative reverse transcription-PCR of splenocyte mRNA (Supplementary Fig. S2A). Analysis of genomic DNA showed that the transgene is the low-affinity FcγRIIIa-F158 allele (Supplementary Fig. S2B).

For the efficacy studies, KPL-4 xenografts were grown in the mammary fat pads of *FcγRI*$^{-/-}$*FcγRIII*$^{-/-}$*RAG2*$^{-/-}$*Tg* (human FcγRIIIa) mice until the tumor size reached an average of 125 mm^3. At this point (day 0), mice were randomly grouped for treatment regimens (n = 9) and treated with single 1 or 3 mg/kg i.v. doses of trastuzumab, afucosylated trastuzumab, or vehicle. Afucosylated trastuzumab inhibited the growth of KPL-4 tumors more effectively than trastuzumab (Fig. 3B, left). Treatment with 3 mg/kg of trastuzumab caused a significant delay in tumor progression (P = 0.003; log rank test; Fig. 3B, right) and the efficacy of afucosylated trastuzumab was significantly improved compared with trastuzumab (P = 0.010; Fig. 3B, right). The median progression-free survival more than doubled for mice treated with afucosylated trastuzumab, compared with treatment with trastuzumab (48 versus 23.4 days, respectively; Fig. 3B, right).

We performed similar experiments using *FcγRI*$^{-/-}$*FcγRIII*$^{-/-}$*RAG2*$^{-/-}$ mice without the human transgene. The KPL-4 tumors were treated with three weekly 3 mg/kg i.v. doses of the antibodies. No significant difference was observed in the response to the antibodies, demonstrating that the increase in the efficacy detected for afucosylated trastuzumab was mediated by the human FcγRIIIa transgene (Fig. 3C).

To ensure that the observed increase in efficacy was not model-dependent, the study was repeated using established MCF7-neo/HER2 xenografts grown in *FcγRI*$^{-/-}$*FcγRIII*$^{-/-}$*RAG2*$^{-/-}$*Tg* (human FcγRIIIa) mice. Similar to KPL-4, these cells overexpress HER2 but do not respond to trastuzumab *in vitro* in a proliferation assay. Again, afucosylated trastuzumab was more potent than trastuzumab in treating MCF7-neo/HER2 tumors, causing four complete responses and five partial responses (Fig. 3D). In contrast, no complete responses and only one partial response was detected in trastuzumab-treated mice. Taken together, these results show that the *in vivo* efficacy of afucosylated trastuzumab is superior to trastuzumab in treating two preclinical models of HER2-amplified breast cancer.

Discussion

It has been hypothesized that ADCC is a general mechanism of action for many therapeutic antibodies (32). However, it remains unclear whether ADCC or the engagement of Fcγ receptors significantly contribute to trastuzumab's antitumor effects in patients with breast cancer. After the initial *in vitro* findings, Ravetch and colleagues showed the *in vivo* importance of FcγR-mediated activity of trastuzumab (13). Notably, these studies did not address the role of FcγR interaction in models with established tumors. Instead, treatments were simultaneous with cell inoculation and thus the results might portray the role of effector cell functions on tumor implantation rather than its effect on solid tumor mass. Our findings confirm the results of Clynes and colleagues and extend them to the treatment of pre-established solid tumors.

The ability to increase *in vitro* ADCC by antibody engineering is widely established (33, 34). However, to our knowledge, it has not been previously shown that the increase in antibody-FcγR interaction leads to increased *in vivo* efficacy in the treatment of established nonhematologic tumors. To directly address this question, we generated afucosylated trastuzumab. The approach was selected primarily because the affinity increase is significant and selective for FcγRIII. Moreover, the variant can be readily produced and is completely devoid of fucose. Fucose in the oligosaccharide (at Asn^{297}) of IgG$_1$ hinders the interaction between carbohydrate of FcγRIIIa (at Asn^{162}) and regions of IgG$_1$ (35). Afucosylation results in increased affinity of the FcγR-IgG$_1$ interaction. The higher affinity observed by afucosylation is selective for human FcγRIIIa and FcγRIIIb because the other human FcγRs are not glycosylated at the corresponding position (35). Therefore, removing the fucose residue results in increased affinity selectively for FcγRIII but not for other FcγR, FcRn, or C1q (23).

We produced afucosylated trastuzumab in *FUT8*$^{-/-}$ CHO cells (30). One alternative technology to produce afucosylated antibodies in CHO cells is to overexpress GnTIII and ManII (35). Interestingly, the clearance of afucosylated trastuzumab was slightly faster than the clearance of trastuzumab in the transgenic mouse model. Hypothetically, the faster clearance might be a result of differential biodistribution leading to the enrichment of antibodies to immune effector cell–rich organs due to increased FcγRIII affinity. Using a mouse model that expresses a human FcγRIIIa transgene in effector cells, we were able to successfully show that an increase in affinity to FcγRIII results in improved efficacy when treating solid tumors. As with any preclinical finding, confirmation of these results will require validation in human clinical trials.

The superior efficacy of afucosylated trastuzumab is not explained by an increase in antibody exposure. However, a plausible mechanism for more effective tumor growth inhibition may be due to the observation that afucosylated antibodies could escape the inhibitory effect of serum IgG. Reports by Iida and colleagues show that serum IgG markedly inhibits the efficacy of rituximab to deplete B cells (36). This inhibition has been attributed to the ability of IgG to compete for FcγRIII binding. However, due to its higher affinity for FcγRIII, afucosylated IgG might escape the inhibitory effect of serum IgG (36–38).

The differential expression of HER2 in tumors relative to normal tissue is thought to account for Herceptin's favorable safety profile. The activity of trastuzumab in ADCC assays is also specific for only high HER2-expressing target cells (11). To maintain this safety profile, it is critical that any increase in ADCC activity does not result in the cytotoxicity of cells that express normal levels of HER2. Previous reports suggest that low-fucose IgG$_1$s could mediate ADCC at low antigen densities at which their corresponding high-fucose counterparts do not induce ADCC (39). However, our ADCC analysis using MCF-10A cells (commonly used as a model for nontransformed low HER2-expressing mammary epithelial cells) failed to detect any significant ADCC using afucosylated trastuzumab.

Published OnlineFirst May 18, 2010; DOI: 10.1158/0008-5472.CAN-09-3704

Because trastuzumab does not bind to murine ErbB2 (HER2), the mouse model used in efficacy studies is not suitable for safety studies. However, more detailed safety studies in non-human primates are required. In conclusion, our results support the development of effector function–enhanced antibodies for solid tumor therapy.

Disclosure of Potential Conflicts of Interest

All authors are employees of Genentech, Inc.

Acknowledgments

We thank Dr. Allen Nguyen for HER2 binding ELISA, and Dr. Pablo Umaña and Dr. Melissa Junttila for discussions and critical review of the manuscript. FcγRI/III double knockout mice were provided by J. Sjef Verbeek, Leiden University Medical Center, Leiden, the Netherlands. Human FcγRIIIa transgenic mice were provided by Jeffrey V. Ravetch, Rockefeller University, New York, NY.

The costs of publication of this article were defrayed in part by the payment of page charges. This article must therefore be hereby marked *advertisement* in accordance with 18 U.S.C. Section 1734 solely to indicate this fact.

Received 10/06/2009; revised 02/22/2010; accepted 03/16/2010; published OnlineFirst 05/18/2010.

References

1. Slamon DJ, Leyland-Jones B, Shak S, et al. Use of chemotherapy plus a monoclonal antibody against HER2 for metastatic breast cancer that overexpresses HER2. N Engl J Med 2001;344:783–92.
2. Cobleigh MA, Vogel CL, Tripathy D, et al. Multinational study of the efficacy and safety of humanized anti-HER2 monoclonal antibody in women who have HER2-overexpressing metastatic breast cancer that has progressed after chemotherapy for metastatic disease. J Clin Oncol 1999;17:2639–48.
3. Vogel CL, Cobleigh MA, Tripathy D, et al. Efficacy and safety of trastuzumab as a single agent in first-line treatment of HER2-overexpressing metastatic breast cancer. J Clin Oncol 2002;20:719–26.
4. Smith I, Procter M, Gelber RD, et al. 2-year follow-up of trastuzumab after adjuvant chemotherapy in HER2-positive breast cancer: a randomised controlled trial. Lancet 2007;369:29–36.
5. Junttila TT, Akita RW, Parsons K, et al. Ligand-independent HER2/HER3/PI3K complex is disrupted by trastuzumab and is effectively inhibited by the PI3K inhibitor GDC-0941. Cancer Cell 2009;15:429–40.
6. Lane HA, Beuvink I, Motoyama AB, Daly JM, Neve RM, Hynes NE. ErbB2 potentiates breast tumor proliferation through modulation of p27(Kip1)-Cdk2 complex formation: receptor overexpression does not determine growth dependency. Mol Cell Biol 2000;20:3210–23.
7. Lee H, Akita RW, Sliwkowski MX, Maihle NJ. A naturally occurring secreted human ErbB3 receptor isoform inhibits heregulin-stimulated activation of ErbB2, ErbB3, and ErbB4. Cancer Res 2001;61:4467–73.
8. Yakes FM, Chinratanalab W, Ritter CA, King W, Seelig S, Arteaga CL. Herceptin-induced inhibition of phosphatidylinositol-3 kinase and Akt is required for antibody-mediated effects on p27, cyclin D1, and antitumor action. Cancer Res 2002;62:4132–41.
9. Molina MA, Codony-Servat J, Albanell J, Rojo F, Arribas J, Baselga J. Trastuzumab (herceptin), a humanized anti-Her2 receptor monoclonal antibody, inhibits basal and activated Her2 ectodomain cleavage in breast cancer cells. Cancer Res 2001;61:4744–9.
10. Pegram M, Hsu S, Lewis G, et al. Inhibitory effects of combinations of HER-2/neu antibody and chemotherapeutic agents used for treatment of human breast cancers. Oncogene 1999;18:2241–51.
11. Lewis GD, Figari I, Fendly B, et al. Differential responses of human tumor cell lines to anti-p185HER2 monoclonal antibodies. Cancer Immunol Immunother 1993;37:255–63.
12. Aguilar Z, Akita RW, Finn RS, et al. Biologic effects of heregulin/neu differentiation factor on normal and malignant human breast and ovarian epithelial cells. Oncogene 1999;18:6050–62.
13. Clynes RA, Towers TL, Presta LG, Ravetch JV. Inhibitory Fc receptors modulate *in vivo* cytoxicity against tumor targets. Nat Med 2000;6:443–6.
14. Musolino A, Naldi N, Bortesi B, et al. Immunoglobulin G fragment C receptor polymorphisms and clinical efficacy of trastuzumab-based therapy in patients with HER-2/neu-positive metastatic breast cancer. J Clin Oncol 2008;26:1789–96.
15. Weng WK, Levy R. Two immunoglobulin G fragment C receptor polymorphisms independently predict response to rituximab in patients with follicular lymphoma. J Clin Oncol 2003;21:3940–7.
16. Arnould L, Gelly M, Penault-Llorca F, et al. Trastuzumab-based treatment of HER2-positive breast cancer: an antibody-dependent cellular cytotoxicity mechanism? Br J Cancer 2006;94:259–67.
17. Gennari R, Menard S, Fagnoni F, et al. Pilot study of the mechanism of action of preoperative trastuzumab in patients with primary operable breast tumors overexpressing HER2. Clin Cancer Res 2004;10:5650–5.
18. Varchetta S, Gibelli N, Oliviero B, et al. Elements related to heterogeneity of antibody-dependent cell cytotoxicity in patients under trastuzumab therapy for primary operable breast cancer overexpressing Her2. Cancer Res 2007;67:11991–9.
19. Nimmerjahn F, Ravetch JV. Divergent immunoglobulin G subclass activity through selective Fc receptor binding. Science 2005;310:1510–2.
20. Stavenhagen JB, Gorlatov S, Tuaillon N, et al. Fc optimization of therapeutic antibodies enhances their ability to kill tumor cells *in vitro* and controls tumor expansion *in vivo* via low-affinity activating Fcγ receptors. Cancer Res 2007;67:8882–90.
21. Kurebayashi J, Otsuki T, Tang CK, et al. Isolation and characterization of a new human breast cancer cell line, KPL-4, expressing the Erb B family receptors and interleukin-6. Br J Cancer 1999;79:707–17.
22. Papac DI, Briggs JB, Chin ET, Jones AJ. A high-throughput microscale method to release *N*-linked oligosaccharides from glycoproteins for matrix-assisted laser desorption/ionization time-of-flight mass spectrometric analysis. Glycobiology 1998;8:445–54.
23. Shields RL, Lai J, Keck R, et al. Lack of fucose on human IgG1 N-linked oligosaccharide improves binding to human Fcγ RIII and antibody-dependent cellular toxicity. J Biol Chem 2002;277:26733–40.
24. Idusogie EE, Presta LG, Gazzano-Santoro H, et al. Mapping of the C1q binding site on rituxan, a chimeric antibody with a human IgG1 Fc. J Immunol 2000;164:4178–84.
25. Munson PJ, Rodbard D. Ligand: a versatile computerized approach for characterization of ligand-binding systems. Anal Biochem 1980;107:220–39.
26. Hazenbos WL, Gessner JE, Hofhuis FM, et al. Impaired IgG-dependent anaphylaxis and Arthus reaction in Fcγ RIII (CD16) deficient mice. Immunity 1996;5:181–8.
27. Ioan-Facsinay A, de Kimpe SJ, Hellwig SM, et al. FcγRI (CD64) contributes substantially to severity of arthritis, hypersensitivity responses, and protection from bacterial infection. Immunity 2002;16:391–402.
28. Li M, Wirthmueller U, Ravetch JV. Reconstitution of human Fc γ RIII cell type specificity in transgenic mice. J Exp Med 1996;183:1259–63.
29. Nguyen A, Reyes AE II, Zhang M, et al. The pharmacokinetics of an albumin-binding Fab (AB.Fab) can be modulated as a function of affinity for albumin. Protein Eng Des Sel 2006;19:291–7.
30. Yamane-Ohnuki N, Kinoshita S, Inoue-Urakubo M, et al. Establishment of FUT8 knockout Chinese hamster ovary cells: an ideal host cell line for producing completely defucosylated antibodies with enhanced antibody-dependent cellular cytotoxicity. Biotechnol Bioeng 2004;87:614–22.
31. Wright A, Morrison SL. Effect of C2-associated carbohydrate

Published OnlineFirst May 18, 2010; DOI: 10.1158/0008-5472.CAN-09-3704

structure on Ig effector function: studies with chimeric mouse-human IgG1 antibodies in glycosylation mutants of Chinese hamster ovary cells. J Immunol 1998;160:3393–402.

32. Adams GP, Weiner LM. Monoclonal antibody therapy of cancer. Nat Biotechnol 2005;23:1147–57.

33. Desjarlais JR, Lazar GA, Zhukovsky EA, Chu SY. Optimizing engagement of the immune system by anti-tumor antibodies: an engineer's perspective. Drug Discov Today 2007;12:898–910.

34. Jefferis R. Glycosylation as a strategy to improve antibody-based therapeutics. Nat Rev Drug Discov 2009;8:226–34.

35. Ferrara C, Stuart F, Sondermann P, Brunker P, Umana P. The carbohydrate at FcγRIIIa Asn-162. An element required for high affinity binding to non-fucosylated IgG glycoforms. J Biol Chem 2006;281:5032–6.

36. Iida S, Misaka H, Inoue M, et al. Nonfucosylated therapeutic IgG1 antibody can evade the inhibitory effect of serum immunoglobulin G on antibody-dependent cellular cytotoxicity through its high binding to FcγRIIIa. Clin Cancer Res 2006;12:2879–87.

37. Preithner S, Elm S, Lippold S, et al. High concentrations of therapeutic IgG1 antibodies are needed to compensate for inhibition of antibody-dependent cellular cytotoxicity by excess endogenous immunoglobulin G. Mol Immunol 2006;43:1183–93.

38. Vugmeyster Y, Howell K. Rituximab-mediated depletion of cynomolgus monkey B cells *in vitro* in different matrices: possibleinhibitory effect of IgG. Int Immunopharmacol 2004;4:1117–24.

39. Niwa R, Sakurada M, Kobayashi Y, et al. Enhanced natural killer cell binding and activation by low-fucose IgG1 antibody results in potent antibody-dependent cellular cytotoxicity induction at lower antigen density. Clin Cancer Res 2005;11:2327–36.

AACR American Association for Cancer Research

Cancer Research

The Journal of Cancer Research (1916–1930) | The American Journal of Cancer (1931–1940)

Superior *In vivo* Efficacy of Afucosylated Trastuzumab in the Treatment of HER2-Amplified Breast Cancer

Teemu T. Junttila, Kathryn Parsons, Christine Olsson, et al.

Cancer Res 2010;70:4481-4489. Published OnlineFirst May 18, 2010.